

The color and stability of Maya Blue: TDDFT calculations

Journal:	<i>The Journal of Physical Chemistry</i>
Manuscript ID:	jp-2008-10945a.R1
Manuscript Type:	Article
Date Submitted by the Author:	28-Mar-2009
Complete List of Authors:	Tilocca, Antonio; University College London, Chemistry Fois, Ettore; Università degli Studi dell'Insubria, DSCA



The color and stability of Maya Blue: TDDFT calculations

Antonio Tilocca ^{a,*} and Ettore Fois ^b^a Department of Chemistry and Materials Simulation Laboratory, University College London, London WC1H 0AJ, U.K.^b DSCA, Università dell'Insubria and INSTM, I-22100 Como, Italy**Abstract**

Car-Parrinello structural optimizations of realistic models of the Maya Blue (MB) hybrid material are combined with TDDFT calculations of the electronic excitation spectra, in order to identify the nature of the fundamental guest-host interactions leading to the unusual stability of this pigment. The comparison with the features of the experimental visible spectrum reveals that the main mode of interaction between the host solid (the palygorskite clay) and the guest molecule (the organic indigo dye) involves the coordination of the carbonyl group of the dye by Al³⁺ ions exposed at the edge of the palygorskite tunnels. Analogous Mg²⁺-dye interactions which do not strongly affect the MB visible spectrum can also be present. Thermal treatment used in the preparation of the pigment appears therefore essential to release some of the structural water molecules tightly bound to the Al³⁺ ions in the internal clay surface, thus leaving them available to coordinate the organic molecule. Moderate heating also favors the oxidation of indigo to dehydroindigo (DHI): the spectral features of the latter complex with Al³⁺ are in remarkable agreement with the experimental spectrum, thus confirming the substantial role of DHI in the properties of Maya Blue.

Keywords: Maya Blue. Hybrid Materials. Indigo. Palygorskite. Time-Dependent Density Functional Theory. Molecular Dynamics Simulations. Car-Parrinello.

* Corresponding author: a.tilocca@ucl.ac.uk

1 Introduction

The intriguing properties of Maya Blue (MB) pigments have attracted considerable interest in the last few years.¹⁻⁵ MB was created around the V century by the ancient Maya civilization, and widely used in Central America until the XVI century. Unlike other non-metallic dyes, the color of artifacts (mural paintings, pottery, statues) painted with MB did not fade and was preserved remarkably well after centuries of exposure to harsh environmental conditions. Laboratory tests have highlighted the unusual resistance of the MB pigment to chemical attack from different sources:⁶ no significant degradation of the vivid MB color is produced either by oxidizing or reducing agents or by concentrated acids, alkalis and organic solvents, or even by high-intensity light sources.⁷ Understanding the basis of this unusual stability could support the development of a new class of environmentally benign colorants, free from heavy metals, and is also an important challenge in order to explore the nature of guest-host interactions in hybrid materials. MB can in fact be considered an inorganic-organic hybrid material:³ it is well established that the Maya craftsmen, anticipating modern synthetic methodologies, prepared this remarkable pigment by combining the indigo organic dye, extracted from several plants, with the palygorskite phyllosilicate clay, using heat to modulate the color and achieve the characteristic MB turquoise-greenish hue: a synthetic equivalent of MB can in fact be prepared in the laboratory through these processes.^{1,8} Because the MB color essentially comes from the indigo dye, it is clear that the association with the palygorskite mineral is crucial to protect the organic molecule and provide the long-term stability of the pigment. A large number of experimental and theoretical investigations have been aimed at elucidating the exact nature of the indigo-palygorskite interaction leading to “mineralization” of indigo. Palygorskite is an hydrated silicate clay, characterized by T:O:T ribbons comprised of an Mg/Al octahedral (O) layer sandwiched between two tetrahedral (T) silicate sheets; inversion of the the apices of the tetrahedra in adjacent ribbons leads to discontinuous O layers, with the formation of porous tunnels running along the *c* crystallographic direction (Figure 1). Each Mg and Al ion at the edge of the tunnels completes its octahedral coordination by bonding two structural water molecules, whereas additional zeolitic water molecules in the channels are only weakly bound. The cross-section of the channels ($3.4 \times 6.4 \text{ \AA}^2$) suggests that the planar indigo molecule (approximate dimension $4.8 \times 12 \text{ \AA}^2$) could fit well within the palygorskite pores, with its main axis roughly aligned along *c*.⁹ This pos-

1
2 sibility was confirmed by Molecular Dynamics simulations,¹⁰ which showed that the indigo molecule migrates in
3
4 the channels until it reaches stable sites, where it is stabilized and held in place by either accepting a hydrogen
5
6 bond from a structural water or forming a direct bond with a clay octahedral cation, both interactions involving
7
8 the molecule's C=O functional group; the MD simulations showed no evidence of Hb's between the indigo amino
9
10 group and structural water. Further static computational investigations and experimental studies (IR, Raman and
11
12 NMR spectroscopy) confirmed that the indigo molecule enters the palygorskite channels, where it interacts mostly
13
14 through its carbonyl group, whereas no strong (Indigo)N-H...O(structural water) bonds were detected.^{11,12} The
15
16 presence of indigo within the channels was also indicated by a periodic superlattice structure extending for 14 Å,
17
18 covering approximately three palygorskite unit cells superimposed along *c*;² powder synchrotron diffraction mea-
19
20 surements did confirm the insertion of indigo, even though they did not find evidence of a superstructure, due to the
21
22 positional and orientational disorder affecting indigo adsorption within the channels.¹³ Another indication of the
23
24 penetration of indigo inside the palygorskite pores was provided by the electrochemical response of MB-analogous
25
26 complexes formed by indigo and either palygorskite or the structurally related sepiolite clay,¹⁴ which denoted a
27
28 much larger depth of penetration of the dye molecule in palygorskite; this explains the lower resistance to acid
29
30 attack of the corresponding MB sepiolite complex, where the adsorbed dye is not protected as effectively as in
31
32 palygorskite.⁶ In fact, the possibility that the dye is adsorbed by hydrogen bonds to the silanol groups on the ex-
33
34 ternal surface of the clay^{7,16} seems more likely for sepiolite-indigo than for palygorskite-indigo complexes, even
35
36 though some experimental data also show that at least a fraction of the dye molecule fills the sepiolite channels as
37
38 well.^{15,17} The observed loss of microporosity upon mixing palygorskite with indigo¹⁶ is certainly compatible with
39
40 the intercalation of the dye within the channels; moreover, whereas thermal treatment is apparently not needed to
41
42 stabilize sepiolite-indigo adducts, it does dramatically improve the stability of indigo-palygorskite MB,¹⁶ which
43
44 can again be correlated to the penetration of indigo in the channels upon loss of zeolitic and structural water. Be-
45
46 sides this evidence, the huge resistance of palygorskite-indigo MB to heat, humidity and chemical attacks, with no
47
48 loss of the radiant color created by thermal treatment, seems much less compatible with models in which the dye
49
50 is attached to the external surface through hydrogen bonds only, also considered the low dye content of MB: the
51
52
53
54
55
56
57
58
59
60

1
2 much more effective protection provided when the dye is adsorbed inside the pores appears necessary to explain
3
4 these properties.
5

6
7 The special turquoise-greenish hues of MB pigment also reflect strong guest-host interactions: heating the indigo-
8
9 palygorskite mixture above 100°C results in the color of the pigment changing from blue (typical of solid indigo) to
10
11 turquoise-greenish.¹⁸ As this mild heat treatment appears essential to produce the high stability of the pigment,¹ it
12
13 seems quite plausible that the same interactions responsible for the color shift are also involved in the stabilization
14
15 of the complex. An immediate effect of heating is the progressive dehydration of palygorskite: zeolitic water
16
17 molecules are lost between room temperature and 130°C, followed by tightly bound structural water which is
18
19 released between 130° and 270°C.¹⁹ Loss of zeolitic water is a necessary step to create room for the bulky indigo
20
21 molecules in the channels; at the same time, the temperature ranges above entail that some structural water can also
22
23 be released during a moderate thermal treatment. Therefore, in addition to H-bonds with structural water, indigo
24
25 can directly interact with the octahedral cations at the edge of the clay inner walls, left exposed after release of
26
27 structural water. The observed red-shift of the C=O stretching frequency observed in experimental FT-IR and FT-
28
29 Raman spectra,^{11,12} indicative of strong guest-host interactions involving the indigo carbonyl, can be interpreted
30
31 as the oxygen either accepting a hydrogen bond or forming a direct metal-oxygen interaction; MD simulations did
32
33 confirm that both these interactions can be important,¹⁰ and either one could in principle be responsible for the
34
35 chemical stability and the optical properties of the MB pigment.
36
37
38
39

40
41 To complete the picture, recent electrochemical data have clearly revealed the presence in the palygorskite matrix
42
43 of dehydroindigo (DHI), which is formed by oxidation of indigo, presumably during the thermal treatment, and
44
45 could also play an important role in the optical properties of MB.²⁰
46
47

48
49 Despite these important findings, identifying the exact nature of the effects leading to the unusual properties of
50
51 Maya Blue remains a challenge, mainly because of the difficulty to separate the individual contributions and iden-
52
53 tify the specific role of several possible guest-host interactions. Given the correlation between color change and
54
55 stability of the pigment, a convenient approach to tackle this intriguing problem involves looking at the *individual*
56
57 effect that different modes of interaction would have on the optical spectrum of MB, in order to identify the role
58
59
60

1
2 of that specific interaction in the overall picture. Ab-initio calculations based on the time-dependent density func-
3 tional theory (TDDFT) formalism²¹ provide very accurate electronic spectra, and can be efficiently combined with
4 structural relaxations of periodic supercells, performed with the Car-Parrinello (CP) method,²² in order to obtain
5 the absorption spectrum of complex systems.^{23,24} In this work we present the results of CP-TDDFT calculations of
6 model systems representing several possible interactions of the MB pigment; the comparison of the optical spectra
7 of these representative models with the experimental spectrum of MB provides new insight into the fundamental
8 effects at the basis of the unusual properties of the pigment.
9
10
11
12
13
14
15
16
17
18
19

20 **2 Computational Methods**

21
22 The TDDFT calculation of electronic absorption spectra of relatively large periodic supercells is currently pro-
23 hibitive even with state-of-the-art computational methods and resources. An attractive alternative consists in per-
24 forming the TDDFT calculation on a smaller subsystem extracted from the extended structure, previously optimized
25 at the DFT level:²⁴ following this approach, we have carried out structural optimizations of several palygorskite-
26 indigo complexes, each one involving a different mode of interaction between the organic dye and the inorganic
27 clay. In particular, we have considered three possible structures involving an indigo molecule interacting with the
28 clay through its carbonyl group: accepting a H-bond from a structural water (model I1); bonded to an Mg²⁺ (model
29 I2), or to an Al³⁺ (model I3) at the edge of the channel. Additionally, we have studied analogous configurations
30 DHI1, DHI2 and DHI3 with an adsorbed dehydroindigo molecule replacing indigo, in order to examine in detail
31 the contribution of DHI to the optical spectrum of MB. The models take into account both possible modes of in-
32 teraction of the indigo carbonyl with the clay discussed before, that is, H-bond to a structural water and direct
33 coordination to an Mg or Al ion; models analogous to I1 and DH1 but involving the indigo amino- instead of the
34 carbonyl group were not considered, because, as mentioned in the Introduction, no clear-cut experimental or theo-
35 retical evidence supports the existence of strong interactions between these groups and structural water molecules,
36 presumably reflecting the unfavorable arrangement of the latter, with the oxygen lone pairs oriented towards the
37 octahedral cation and the protons pointing towards the channel, which does not allow the formation of strong Hbs
38
39
40
41
42
43
44
45
46
47
48
49
50
51
52
53
54
55
56
57
58
59
60

1
2 with the indigo NH.^{10,11}

3
4 Figure 2 illustrates the procedure followed to obtain the input models for the TDDFT calculations. An $1 \times 1 \times$
5
6
7
8
9
10
11
12
13
14
15
16
17
18
19
20
21
22
23
24
25
26
27
28
29
30
31
32
33
34
35
36
37
38
39
40
41
42
43
44
45
46
47
48
49
50
51
52
53
54
55
56
57
58
59
60

3 monoclinic palygorskite supercell was created using the experimental atomic coordinates;²⁵ the composition of the unit cell was $\text{Si}_{16}\text{Mg}_4\text{Al}_4[\text{O}_{40}(\text{OH})_4(\text{H}_2\text{O})_8] \cdot 8\text{H}_2\text{O}$, with structural water inside the brackets and weakly bound water outside; equal Mg:Al occupancy in the octahedral layers was assumed. The $1 \times 1 \times 3$ supercell contains two parallel channels extending for 15.1 Å along *c*. In order to make room for the organic molecule, all zeolitic water molecules were removed from one of the two channels, mimicking the effect of the mild thermal treatment used in MB preparation. For model I1, an indigo molecule was then inserted in the half-empty channel, in a stable H-bonded configuration previously identified through classical MD simulations at room temperature;¹⁰ ab-initio structural optimization of the resulting indigo-clay complex (see below) followed. To prepare models I2 and I3, in addition to zeolitic water, all structural water molecules bound to the octahedral Mg (Al) ions on one side of the channel were also removed, and an indigo molecule bound to one of the now exposed Mg^{2+} or Al^{3+} was inserted, again in an initial geometry extracted from previous classical MD simulations.¹⁰ Each of these initial indigo-palygorskite complexes was then locally optimized by damped Car-Parrinello Molecular Dynamics (CPMD), using a plane wave basis set with the PBE exchange-correlation functional²⁶ and ultrasoft pseudopotentials,²⁷ until the largest component of the ionic forces was lower than 0.025 eV/Å.²⁸ Further CPMD runs of ~ 5 ps at room temperature were carried out on each of the six periodic models of MB, to check the stability of the structure. Having obtained realistic periodic structures, a small model representative of the underlying indigo-palygorskite interaction was extracted in each case from the extended structure, by taking the indigo molecule and the palygorskite interaction sites closest to the indigo five-ring chromophore units containing the carbonyl interaction sites (Figure 2). Model I1, featuring the $\text{C}=\text{O} \cdots \text{H}-\text{O}-\text{H}$ hydrogen bond, included indigo, four structural water molecules and an Mg^{2+} ; models I2 (I3) contained the Mg^{2+} (Al^{3+}) ion directly bound to the indigo $\text{C}=\text{O}$, plus the four oxygen atoms in the Mg (Al) coordination shell, which were saturated by adding H atoms located along the dangling O(-Si) bonds resulting from the cut. This procedure resulted in models I2 and I3 containing four water molecules and a two- or tri-valent cation in addition to the indigo molecule, as for model I1. In order to obtain

1
2 the DHI, DH2 and DH3 models, indigo was replaced with dehydroindigo in the corresponding optimized periodic
3
4 structure, and the structural minimization was restarted, leading to the extended models of the DHI-palygorskite
5
6 interaction, from which the sub-systems for the TDDFT calculations were extracted exactly as done for indigo.
7
8 The 25 lowest excitations of each model were calculated via TDDFT, using the Gaussian98 code²⁹ with the B3LYP
9
10 functional³⁰ and an all-electron 6-311+G(2d,p) basis; this computational setup has been shown to yield converged
11
12 excitation energies for indigo derivatives.³¹ In order to maintain the electronic and structural effects of the realistic
13
14 local environment in the periodic structures, no further minimization was performed on the models before the
15
16 TDDFT calculations.
17
18
19
20
21
22

23 **3 Results and Discussion**

24
25
26 An important issue to consider first is the adequacy of the specific models of interaction examined in this work. In
27
28 particular, it could be argued that removal of all the structural water molecules in the (DH)I2 and (DH)I3 structures
29
30 is not fully justified, as it is well established that these molecules are removed in two steps, and the full dehydration
31
32 of palygorskite leads to structural collapse which would prevent the dye molecule to reach the octahedral sites left
33
34 exposed at the edge of the channels.^{16,19,36} However, the transformation of palygorskite to a folded phase with
35
36 unaccessible pores only occurs at a temperature 100 K above the loss of all structural water:³⁶ therefore, a model
37
38 in which indigo molecules penetrate the channels upon moderate thermal treatment, which leads to the loss of a
39
40 significant fraction of the structural water, while still keeping the channels intact, seems reasonable, based on the
41
42 experimental data. Interestingly enough, as the driving force for folding is the need to complete the coordination of
43
44 the octahedral cations after losing their bound structural water,³⁶ this may also suggest a role of indigo in inhibiting
45
46 structural folding by propping open the tunnels. Another equally valid possibility, still supporting the (DH)I2 and
47
48 (DH)I3 models, entails indigo displacing structural water in the octahedral coordination shell *before* the water is
49
50 lost in the heating stage, with a mechanism similar to the one highlighted for pyridine intercalated in sepiolite.³⁷ In
51
52 order to assess this possibility, we have performed additional structural optimizations of two isoelectronic periodic
53
54 models of MB with a single structural water in the channel; in the first model, indigo was H-bonded to a structural
55
56
57
58
59
60

1
2 water, coordinated to Al; in the second model, the indigo C=O group was directly bonded to the Al, displacing the
3
4 water molecule which was H-bonded to the second carbonyl. In this way, both models feature the same indigo-water
5
6 H-bond, and any difference in their total energies reflects the different strength of I-Al and H₂O-Al interactions.
7
8 The comparison of the energies of the optimized structures shows that the direct I-Al interaction is 40.5 kJ/mol
9
10 stronger, suggesting that indigo can effectively displace structural water in the octahedral coordination shell during
11
12 heating, and therefore further supporting our models, as not all structural water must be released before the (DH)I2
13
14 and (DH)I3 modes of interaction can be established. As an additional test, all room-temperature CPMD simulations
15
16 of the various structures with indigo or dehydroindigo directly bound to an octahedral cation showed remarkable
17
18 stability, with no structural distortion observed in any case.
19
20
21

22
23 The calculated electronic excitation spectra of the six interaction models are plotted in Figure 3, which also
24
25 shows the experimental optical spectrum of MB¹⁸ and the calculated spectra for isolated indigo and dehydroindigo
26
27 molecules. The 18000 cm⁻¹ lowest energy peak of gas-phase indigo ($\pi \rightarrow \pi^*$ transition) is in excellent agreement
28
29 with the gas-phase value calculated at the same level of theory,³¹ which lies about 300-400 cm⁻¹ below the ex-
30
31 perimental value.^{32,33} Intermolecular interactions such as hydrogen bonds strongly shift this absorption to lower
32
33 energies: the first excitation is found at 16600 cm⁻¹ in polar solvents such as ethanol,³⁴ and further lower (15000
34
35 cm⁻¹) in solid indigo.^{18,35} The strong bathochromic effect seems to result mainly from the stabilization of the ex-
36
37 cited states in a polar environment.³³ In the unheated indigo-palygorskite mixture, the organic dye is mostly found
38
39 in solid clusters on the clay external surface, giving the absorption peak around 15000 cm⁻¹ and the deep blue
40
41 color of solid indigo. The color change to turquoise-green upon thermal treatment is caused by a small blue-shift of
42
43 the lowest energy transition and the appearance of a broad secondary peak centered around 20400 cm⁻¹.¹⁸ These
44
45 shifts clearly suggest a significant change in the molecular environment upon heating, resulting from the penetra-
46
47 tion of the molecule inside the clay channels where zeolitic water has been released. Figure 3 shows that the models
48
49 correctly reproduce the large red-shift of the lowest energy transition of the molecule in MB, with respect to the
50
51 gas-phase. Most importantly, the models allow us to identify the guest-host interaction responsible of the color
52
53 shift, and therefore of the stability of MB.
54
55
56
57
58
59
60

1
2 Based on the match with the first two peaks in the experimental optical spectrum, which as mentioned before
3
4 determine the color shift in MB upon heating, the best models of the dye-clay interaction in MB are DH3 and I3.
5
6 The models of the indigo-palygorskite interaction reproduce the lowest-energy absorption peak reasonably well,
7
8 but only the I3 model with indigo bound to Al also yields a significant contribution in the region of the second
9
10 absorption of MB: for instance, while the I-Mg model yields an almost perfect lowest energy transition at 15600
11
12 cm^{-1} , it does not produce any secondary absorption around 20000-21000 cm^{-1} . Analogously, the DH3 model,
13
14 with the DHI-palygorskite interaction involving Al, yields an optical spectrum much closer to the experimental
15
16 one, as long as the first two MB peaks are concerned: DH3 yields two peaks at 15300 and 20600 cm^{-1} quite
17
18 close to the experiment, whereas the first peak of DH1 and DH2 are less accurate; moreover, both DH1 and DH2
19
20 yield an absorption around 18000 cm^{-1} , which is absent from DH3 and actually correspond to a minimum in the
21
22 experimental spectrum of MB, which is considered critical for the color of the pigment.¹⁸
23
24
25
26

27 Based on these observations, three important remarks can be made:

28
29
30 (i) the direct interaction between the dye and the clay octahedral cations is more important than the hydrogen bond
31
32 with structural water in determining the MB properties: H-bonded models of indigo and dehydroindigo do not
33
34 reproduce either the lowest transition or the broad secondary absorption of the experimental MB spectrum.
35

36
37 (ii) Al^{3+} cations are more likely candidates than Mg^{2+} for directly bonding the dye carbonyl and determining the
38
39 two lowest-energy transitions; at the same time, the peak around 27500 cm^{-1} shows a strong correlation with the
40
41 direct-interaction complexes involving Mg^{2+} . While the latter peak can only have a lower impact on the MB color,
42
43 this effect denotes that Mg^{2+} -indigo and Mg^{2+} -dehydroindigo bonds can still be present in Maya Blue. In practice,
44
45 this means that a fraction of the organic dye can be bonded to Mg, without strongly affecting the color of the
46
47 pigment.
48
49

50
51 (iii) while both indigo and dehydroindigo molecules are involved in the interaction with the host, the models with
52
53 the oxidized dye provide a closer match with experiment, indicating that, after thermal treatment, a significant
54
55 amount of DHI can be present in the MB pigment.²⁰
56
57
58
59
60

4 Conclusions

Using CP-TDDFT calculations to map out the individual contribution of specific guest-host interactions to the optical spectrum of Maya Blue allowed us to make a substantial step towards a fundamental understanding of the unusual properties of this pigment. The most likely association between the organic dye and the inorganic clay turns out to involve Al^{3+} cations, exposed at the edge of the clay tunnels, and the carbonyl group of the adsorbed dye. Mg^{2+} -dye interactions which do not affect the visible spectrum of the pigment can also be present. The spectral features of dehydroindigo are in closer agreement with the experimental pattern than those of indigo, thus supporting the recent suggestion that the oxidized form of indigo yields a substantial contribution to the optical and physico-chemical properties of Maya Blue.²⁰ The role of a moderate thermal treatment in achieving the MB stability is twofold: (i) it will lead to the loss of weakly bound water and of a fraction of the structural water, thus exposing some Al^{3+} ions which can strongly bind the carbonyl of the organic molecule; (ii) it will induce the oxidation of indigo to dehydroindigo, which is thermodynamically favored at higher temperature. The relative distribution of indigo and dehydroindigo in the palygorskite tunnels can also be affected by the different mobility of these species, which presumably results from the higher flexibility of DHI with respect to the central C-C bond: MD simulations at different temperatures could be employed to investigate this issue.

Acknowledgments

This work was partially supported by the HPC-Europa program (project number: 211437) with the support of the European Community - Research Infrastructure Action of the FP7 Programme. A.T. thanks the UK's Royal Society for financial support (University Research Fellowship).

References

- [1] Van Olphen, H. *Science* **1966**, *154*, 645.
- [2] José-Yacamán, M.; Rendón, L.; Arenas, J.; Serra Puche, M. C. *Science* **1996**, *273*, 223.

- 1
2 [3] Romero, P. G.; Sanchez, C. *New J. Chem.* **2005**, *29*, 57.
3
4
5 [4] Berke, H. *Chem. Soc. Rev.* **2007**, *36*, 15.
6
7
8 [5] Arnold, D. E.; Branden, J. R., Williams, P. R. Feinman, G. M.; Brown. J. P. *Antiquity* **2008**, *82*, 151.
9
10
11 [6] Sánchez Del Río, M.; Martinetto, P.; Reyes-Valerio, C.; Dooryhee, E. Suárez, M. *Archaeometry* **2006**, *1*, 115.
12
13
14 [7] Chiari, G.; Giustetto, R.; Druzik, J.; Doehne, E.; Ricchiardi, G. *Appl. Phys. A* **2008**, *90*, 3.
15
16
17 [8] Doménech, A.; Doménech-Carbó, M. T.; Vázquez de Agredos Pascual, M. L. *Anal. Chem.* **2007**, *79*, 2812.
18
19
20 [9] Kleber, R.; Masschelein-Kleiner, R.; Thissen, J. *Studies in Conservation* **1967**, *12*, 41.
21
22
23 [10] Fois, E.; Gamba, A.; Tilocca, A. *Microporous Mesop. Mater.* **2003**, *57*, 263.
24
25
26 [11] Giustetto, R.; Llabres i Xamena, F.; Ricchiardi, G.; Bordiga, S.; Damin, A.; Gobetto, R.; Chierotti, M. R. *J.*
27
28
29 *Phys. Chem. B* **2005**, *109*, 19360.
30
31
32 [12] Manciu, F. S.; Ramirez, A.; Durrer, W.; Govani, J.; Chianelli, R. R. *J. Raman Spectrosc.* **2008**, *39*, 1257.
33
34
35 [13] Chiari, G.; Giustetto, R.; Ricchiardi, G. *Eur. J. Mineral.* **2003**, *15*, 21.
36
37
38 [14] Doménech, A.; Doménech-Carbó, M. T.; Sánchez del Rio, M.; Vázquez de Agredos Pascual, M. L. *J. Solid*
39
40
41 *State Electrochem.* **2009**, *13*, 869.
42
43
44 [15] Ovarlez, S.; Chaze, A. M.; Giulieri, F.; Delamare, F. *C. R. Chimie* **2006**, *9*, 1243.
45
46
47 [16] Hubbard, B.; Kuang, W.; Moser, A.; Facey, G. A.; Detellier, C. *Clays Clay Miner.* **2003**, *3*, 318.
48
49
50 [17] Yasarawanvan, N.; van Duijneveldt, J. S. *Langmuir* **2008**, *24*, 7184.
51
52
53 [18] Reinen, D.; Köhl, P.; Müller, C. *Z. Anorg. All. Chem.* **2004**, *630*, 97.
54
55
56 [19] Kuang, W.; Facey, G. A.; Detellier, C. *Clays Clay Miner.* **2004**, *52*, 635.
57
58
59
60

- 1
2 [20] Doménech, A.; Doménech-Carbó, M. T.; Vázquez de Agredos Pascual, M. L. *J. Phys. Chem. B* **2006**, *110*,
3
4 6027.
5
6
7 [21] Casida, M. E.; Jamorsky, C.; Casida, K. C.; Salahub, D. R. *J. Chem. Phys.* **1998**, *108*, 4439.
8
9
10 [22] Car, R.; Parrinello, M. *Phys. Rev. Lett.* **1985**, *55*, 2471.
11
12
13 [23] De Angelis, F.; Tilocca, A.; Selloni, A. *J. Am. Chem. Soc.* **2004**, *126*, 15024.
14
15
16 [24] Fois, E.; Gamba, A.; Tabacchi, G. *ChemPhysChem* **2005**, *6*, 1237.
17
18
19 [25] Artioli, G.; Galli, E. *Mater. Sci. Forum* **1994**, *647*, 166.
20
21
22 [26] Perdew, J. P.; Burke, K.; Ernzerhof, M. *Phys. Rev. Lett.* **1996**, *77*, 3865.
23
24
25 [27] Vanderbilt, D. *Phys. Rev. B* **1990**, *41*, 7892.
26
27
28 [28] Tilocca, A.; Di Valentin, C.; Selloni, A. *J. Phys. Chem. B* **1995**, *109*, 20963.
29
30
31 [29] *Gaussian98*, revision A.11.3; Frisch, M. J.; Trucks, G. W.; Schlegel, H. B.; Scuseria, G. E.; Robb, M. A.;
32
33 Cheeseman, J. R.; Zakrzewski, V. G.; Montgomery, J. A., Jr.; Stratmann, R. E.; Burant, J. C.; Dapprich,
34
35 S.; Millam, J. M.; Daniels, A. D.; Kudin, K. N.; Strain, M. C.; Farkas, O.; Tomasi, J.; Barone, V.; Cossi,
36
37 M.; Cammi, R.; Mennucci, B.; Pomelli, C.; Adamo, C.; Clifford, S.; Ochterski, J. W.; Petersson, G. A.;
38
39 Ayala, P. Y.; Cui, Q.; Morokuma, K.; Rega, N.; Salvador, P.; Dannenberg, J. J.; Malick, D.; Rabuck, A.
40
41 D.; Raghavachari, K.; Foresman, J. B.; Cioslowski, J.; Ortiz, J. V.; Baboul, A. G.; Stefanov, B. B.; Liu, G.;
42
43 Liashenko, A.; Piskorz, P.; Komaromi, I.; Gomperts, R.; Martin, R. L.; Fox, D. J.; Keith, T.; Al-Laham, M.
44
45 A.; Peng, C. Y.; Nanayakkara, A.; Challacombe, M.; Gill, P. M. W.; Johnson, B.; Chen, W.; Wong, M. W.;
46
47 Andres, J. L.; Gonzalez, C.; Head-Gordon, M.; Replogle, E. S.; Pople, J. A.; Gaussian, Inc.: Pittsburgh, PA,
48
49 2002.
50
51 [30] Becke, A. D. *J. Chem. Phys.* **1993**, *98*, 5648.
52
53
54
55 [31] Jacquemin, D.; Preat, J.; Wathelet, V.; Perpète, E. A. *J. Chem. Phys.* **2006**, *124*, 074104.
56
57
58
59
60

1
2 [32] Sheppard, S. E.; Newsome, P. T. *J. Am. Chem. Soc.* **1942**, *64*, 2937.
3

4
5 [33] Sadler, P. W. *J. Org. Chem.* **1956**, *21*, 316.
6

7
8 [34] Gerke, R.; Fitjer, L.; Müller, P.; Usón, I.; Kowskic, K.; Rademacher, P. *Tetrahedron* **1999**, *55*, 14429.
9

10
11 [35] While head-to-tail dimerization has also been reported to red-shift indigo absorption in the clay sepiolite,¹⁷
12 no such feature has been observed for indigo in palygorskite,¹⁸ presumably due to the narrower channels of
13 palygorskite which prevent dimerization by reducing the translational freedom of indigo monomers.
14
15
16
17

18
19 [36] Post, J. E.; Heaney, P. J. *Am. Miner.* **2008**, *93*, 667.
20

21
22 [37] Facey, G. A.; Kuang, W.; Detellier, C. *J. Phys. Chem. B* **2005**, *109*, 22359.
23
24
25
26
27
28
29
30
31
32
33
34
35
36
37
38
39
40
41
42
43
44
45
46
47
48
49
50
51
52
53
54
55
56
57
58
59
60

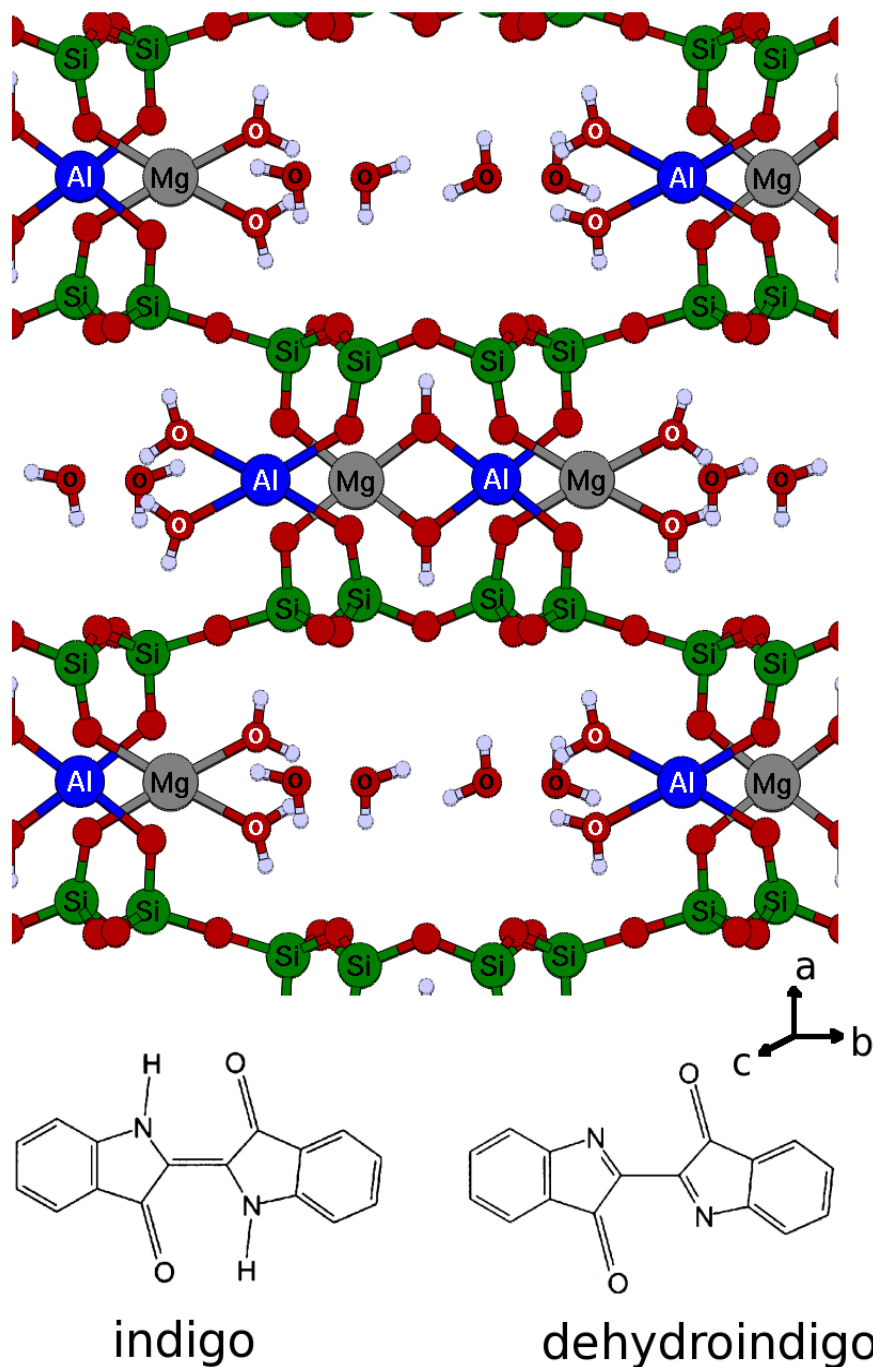


Figure 1: The structure of Maya Blue inorganic and organic components. (top) The palygorskite clay (experimental monoclinic coordinates²⁵): oxygen atoms of tightly bound structural water are labelled in white, whereas the oxygen atoms of zeolitic water bear dark labels; (bottom) chemical structure of indigo and dehydroindigo dyes.

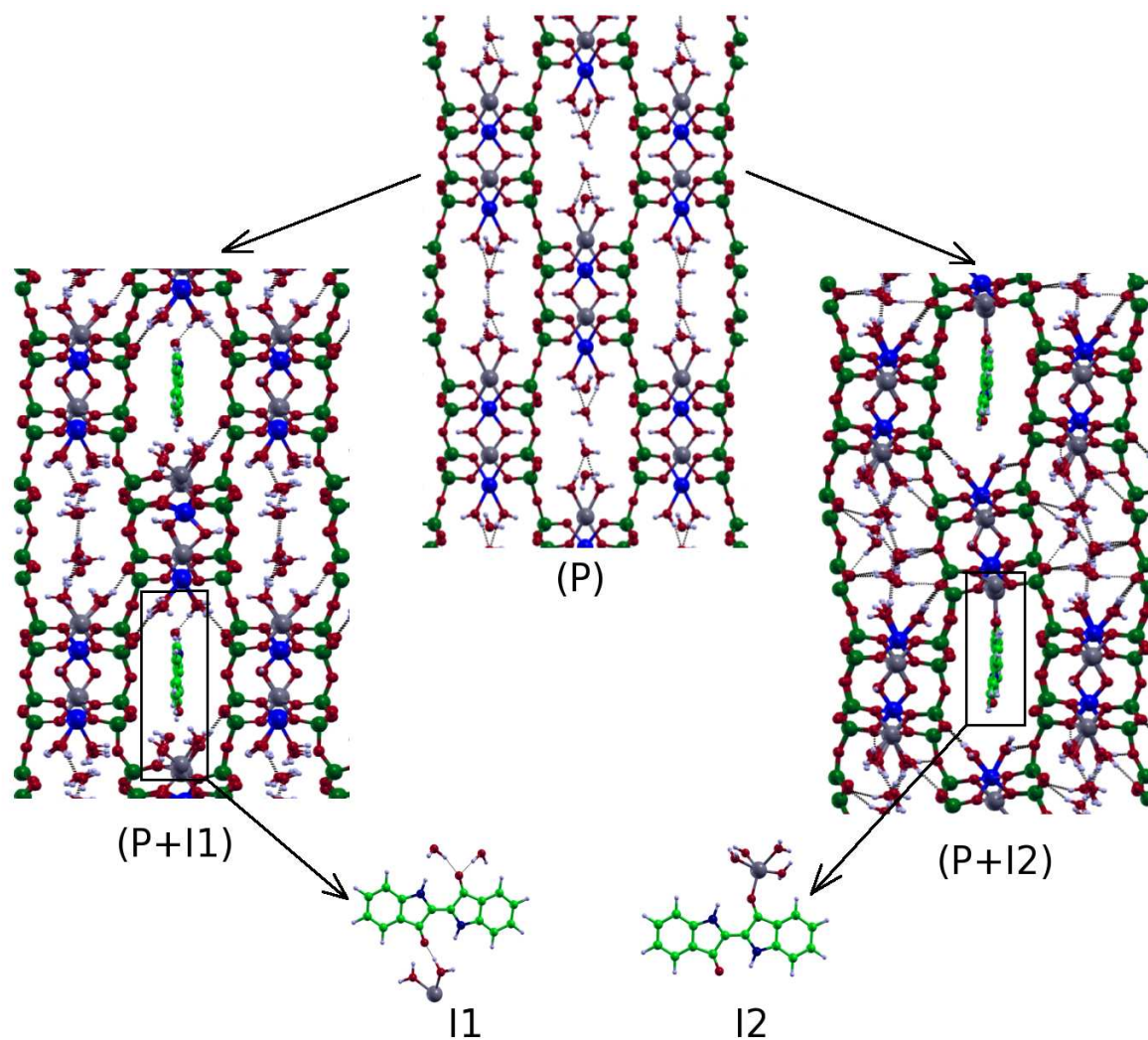


Figure 2: The procedure used to generate small input models for the TDDFT calculations, representative of specific indigo-palygorskite interactions. For model I1, the experimental structure of palygorskite (P) was modified by removing all zeolitic water in a channel, and replacing it with an indigo molecule; structural optimization then led to structure P+I1, from which the indigo molecule and the palygorskite atoms closest to the carbonyl groups were extracted. In the case of models I2-I3, the structural water molecules were also removed from the top of the channel in (P), exposing Mg^{2+} (Al^{3+} for model I3) ions to which the inserted indigo molecule could associate. Structural optimization led to (P+I2), from which model I2 was extracted.

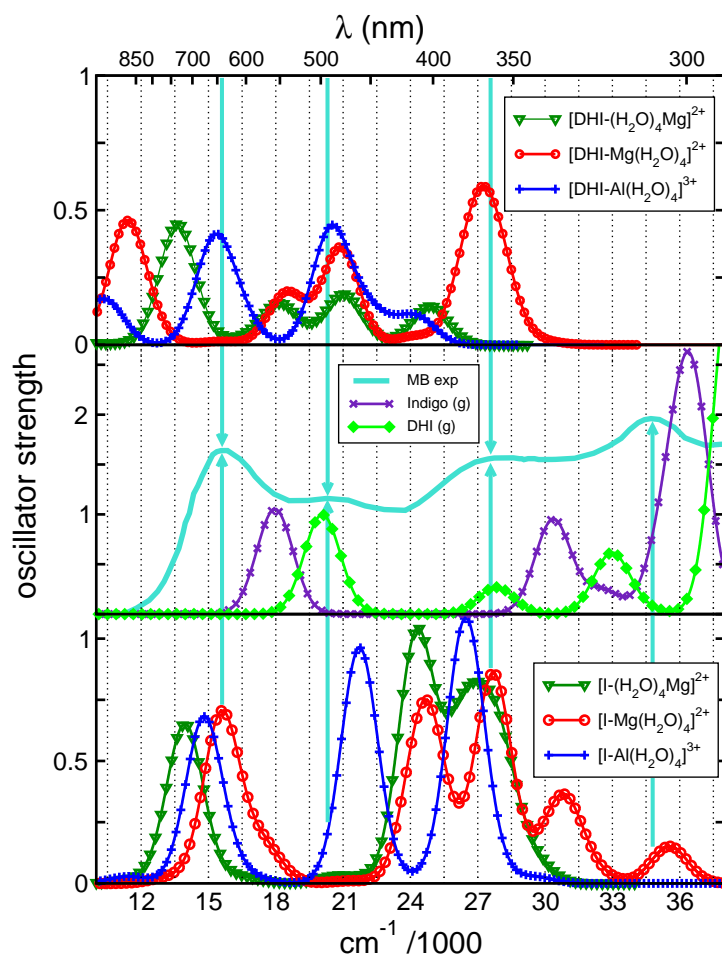


Figure 3: Calculated TDDFT electronic excitation spectra of the palygorskite-indigo (bottom panel) and the palygorskite-dehydroindigo (top panel) models of Maya Blue. The central panel shows the experimental optical spectrum of MB (taken from reference 18) and the calculated spectrum for gas-phase indigo and dehydroindigo. The theoretical spectra were obtained applying a gaussian broadening with $\sigma=0.1$ eV to the TDDFT lowest 25 excitations energies and corresponding oscillator strengths. Vertical arrows are used to mark the main absorption peaks in the experimental spectrum.